Liver Cancer

Research Article

Liver Cancer 2023;12:356–371
DOI: 10.1159/000527498

Received: December 27, 2021
Accepted: September 18, 2022
Published online: January 24, 2023

Contrast-Enhanced Ultrasound Liver Imaging Reporting and Data System in Hepatocellular Carcinoma ≤5 cm: Biological Characteristics and Patient Outcomes

Wen-Jia Cai[a] Minghua Ying[b] Rong-Qin Zheng[c] Jintang Liao[d] Baoming Luo[e] Lina Tang[f] Wen Cheng[g] Hong Yang[h] An Wei[i] Yilin Yang[j] Hui Wang[k] Yan-Chun Luo[a] Cun Liu[l] Hui Zhong[m] Qi Yang[n] Jie Yu[a] Ping Liang[a]

[a]Department of Interventional Ultrasound, Chinese PLA General Hospital, Beijing, China; [b]Department of Diagnostic Ultrasound, Fifth Medical Center of Chinese PLA General Hospital, Beijing, China; [c]Department of Medical Ultrasound, Guangdong Key Laboratory of Liver Disease Research, The Third Affiliated Hospital of Sun Yat-sen University, Guangzhou, China; [d]Department of Diagnostic Ultrasound, Xiangya Hospital Central South University, Changsha, China; [e]Department of Ultrasound, Sun Yat-sen Memorial Hospital, Sun Yat-sen University, Guangzhou, China; [f]Department of Diagnostic Ultrasound, Fujian Cancer Hospital and Fujian Medical University Cancer Hospital, Fuzhou, China; [g]Department of Ultrasound, Harbin Medical University Cancer Hospital, Harbin, China; [h]Department of Medical Ultrasound, The First Affiliated Hospital of Guangxi Medical University, Nanning, China; [i]Department of Interventional Ultrasound, Hunan Provincial People's Hospital, Changsha, China; [j]Department of Ultrasound Diagnosis, Tangdu Hospital, Fourth Military Medical University, Xi'an, China; [k]Department of Ultrasound, China-Japan Union Hospital of Jilin University, Changchun, China; [l]Department of Ultrasound, Jinan Central, Hospital Affiliated to Shandong First Medical University, Jinan, China; [m]Department of Biomedical Engineering, School of Life Science and Technology, Xi'an Jiaotong University, Xi'an, China; [n]Department of Medical Ultrasound, Peking University Shenzhen Hospital, Shenzhen, China

Keywords

Hepatocellular carcinoma · Contrast-enhanced ultrasound · Liver imaging reporting and data system · Prognosis · Ki-67

Abstract

Introduction: The present study aimed to evaluate the influence of biological characteristics of hepatocellular carcinoma (HCC) on the Liver Imaging Reporting and Data System (LI-RADS) v2017 category of contrast-enhanced ultrasound (CEUS) in patients with high risk and compare the outcomes among different categories after radical resection. ***Methods:*** Between June 2017 and December 2020, standardized CEUS data of liver nodules were prospectively collected from multiple centers across China. We conducted a retrospective analysis of the prospectively collected data on HCCs measuring no more than 5 cm, as diagnosed by pathology. LI-RADS categories were assigned after thorough evaluation of CEUS features. Then, CEUS LI-RADS categories and major features were compared in different differentiation, Ki-67, and microvascular invasion (MVI) statuses. Differences in recurrence-free survival (RFS) among different LI-RADS categories were further analyzed. ***Results:*** A total of 293 HCC nodules in 293 patients were included. This study revealed significant differences in the CEUS LI-RADS category of HCCs among differentiation ($p < 0.001$) and levels of Ki-67 ($p = 0.01$) and that poor differentiation (32.7% in LR-M, 12% in LR-5, and 6.2% in LR-4) ($p < 0.001$) and high level of Ki-67 (median value 30%)

Karger@karger.com
www.karger.com/lic

Correspondence to:
Jie Yu, jiemi301@163.com
Ping Liang, liangping301@126.com

were more frequently classified into the LR-M category, whereas well differentiation (37.5% in LR-4, 15.1% in LR-5, and 11.5% in LR-M) and low levels of Ki-67 (median value 11%) were more frequently classified into the LR-4 category. No significant differences were found between MVI and CEUS LI-RADS categories ($p > 0.05$). With a median follow-up of 23 months, HCCs assigned to different CEUS LI-RADS classes showed no significant differences in RFS after resection. ***Conclusions:*** Biological characteristics of HCC, including differentiation and level of Ki-67 expression, could influence major features of CEUS and impact the CEUS LI-RADS category. HCCs in different CEUS LI-RADS categories showed no significant differences in RFS after resection.

Introduction

Non-invasive imaging modalities, mainly including contrast-enhanced magnetic resonance imaging/computed tomography (CE MRI/CT), play a critical role in the diagnosis of hepatocellular carcinoma (HCC) in patients with high risk [1]. Simultaneously, contrast-enhanced ultrasound (CEUS), as a more available and safe method without radiation exposure or nephrotoxicity, has been recommended by many guidelines for diagnosing HCC when CE CT and MRI are inconclusive or contraindicated [2–4]. Furthermore, the CEUS Liver Imaging Reporting and Data System (CEUS LI-RADS) (v2017), expanded from LI-RADS by experts from the American College of Radiology (ACR), has greatly improved the standardization and consistency of evaluation criteria among sonographers [5, 6]. A large retrospective study with more than 1,000 lesions in cirrhosis showed that the LI-RADS 5 classification (LR-5, definition of the typical HCC pattern for CEUS) was highly specific for HCC (with a positive predictive value (PPV) of 98.5%), enabling its application for a confident non-invasive diagnosis [7].

However, CEUS LI-RADS also presented poor sensitivity and accuracy, which hindered it from being recognized as a precise and widely used method in clinical practice [8]. According to previous studies, the CEUS LI-RADS algorithm showed the lowest sensitivity (64%) for the diagnosis of HCC in cirrhotic patients, when compared to a European CEUS algorithm (Erlanger Synopsis for Contrast-Enhanced Ultrasound for Liver Lesion Assessment in Patients at Risk [ESCULAP]) (94.2%) and CEUS on-site (90.9%) ($p < 0.001$) [9]. A previous study also revealed that a large proportion of HCC was categorized into LR-M or 4 categories (44% and 86%, respectively) rather than LR-5 [7]. Therefore, those misclassifications might cause an unnecessary increase in the requirement for further examination, including another imaging or even invasive biopsy to confirm. CEUS LI-RADS categorization is mainly based on major imaging features of CEUS, including the type and degree of arterial phase enhancement and the timing and degree of washout [10]. Some of these imaging features have been proven to be influenced by the biological characteristics of HCC, such as differentiation [11, 12], level of Ki-67 expression [13, 14], or microvascular invasion (MVI) status [15, 16]. However, whether the influence would ultimately affect the CEUS LI-RADS classification has not been determined. We therefore hypothesized that the biological characteristics of HCC impacted the CEUS LI-RADS classification.

Moreover, whether this standardized diagnostic scheme of the CEUS LI-RADS category can be accurately correlated with clinical outcomes and provide guidance on the appropriate management of HCC nodules is not entirely clear. Few previous studies have explored the association between LI-RADS and prognosis; however, most of those studies were based on CT or MRI LI-RADS and showed inconsistent results. In addition, those studies lacked a comprehensive investigation of the biologic characteristics of the index HCC nodules, including differentiation, Ki-67 level, or MVI status, which may impact the outcomes. Therefore, we also tested the hypothesis as to whether HCC nodules assigned to different CEUS LI-RADS categories presented different recurrence-free survival (RFS) after radical resection.

Thus, the purpose of this study was to assess the impact of biological characteristics of HCC (including differentiation, level of Ki-67 expression, and MVI status) on the LI-RADS category based on multicenter CEUS images prospectively collected across China, to further compare the outcomes between different categories after radical resection, and finally to explore possible strategies to improve the precision of LI-RADS classification.

Materials and Methods

Data Source

A prospective nationwide multicenter study was launched on June 25, 2017, in China. The prospectively multicenter study was reviewed and approved by the Ethical Committee of the Chinese PLA General Hospital (S2017-046-03) as the coordinating center; based on this, all other clinical partners received ethical approval

for the study. The prospective study was registered at ClinicalTrials.gov (NCT04682886). Retrospective analysis based on the collected data in this study had been approved by each center and was in line with the Declaration of Helsinki. Data containing US images and/or CEUS videos and clinical information were uploaded into the online database (http://www.usliver.org). In the involved centers, CEUS is routinely performed for further investigation when conventional ultrasound is insufficient to characterize the incidental FLLs. Additionally, in some centers, CEUS is usually completed as a precursor examination before further treatment.

Indications for CEUS in the prospective study were not strictly identical in all centers. In the top 3 hospitals in this study, including The Third Affiliated Hospital of Sun Yat-sen University, Sun Yat-Sen Memorial Hospital of Sun Yat-Sen University, and Xiangya Hospital of Central South University, which accounted for more than two-thirds of the total cases, CEUS is held as a routine standard practice for all significant newly detected non-cystic liver lesion nodules after routine ultrasound. Accordingly, the patient collection in these centers reflected an almost consecutive enrollment. In series from other centers, CEUS is usually used to evaluate liver nodules which are suspected of malignancy, nodules in addition to the already diagnosed liver cancers, or as a precursor examination before biopsy or locoregional therapies. Written informed consent was obtained from participants in this study.

Patients

Between June 2017 and December 2020, all uploaded CEUS data of HCCs diagnosed by resection pathology were retrospectively evaluated. All 293 participants enrolled in this study complied with the same inclusion and exclusion criteria. The inclusion criteria were as follows: (i) HCC with histological diagnosis by resection pathology; (ii) HCC with diameters no more than 5 cm; (iii) presence of identified risk factors for HCC (cirrhosis, chronic hepatitis B viral infection, or current or prior HCC); (iv) CEUS examination within 1 month before resection; and (v) age of at least 18 years. The exclusion criteria included (i) incomplete clinicopathological data and (ii) poor CEUS quality (Fig. 1).

Furthermore, to compare the prognosis in different CEUS LI-RADS classifications, patients with more than one nodule or no primary HCC were excluded to avoid the potential effects of disease severity. Patients lost to follow-up were also excluded. Finally, 208 nodules in 208 patients with single and primary HCC were included in the prognostic analysis (Fig. 1).

All clinical and laboratory information was collected and reviewed from patients' records. The albumin-bilirubin (ALBI) score was computed by the formula 0.085 (albumin g/L) + 0.66 log (bilirubin mol/L). Patients were then stratified into 3 grades: ALBI grade 1 (≤2.60), grade 2 (>2.60 to 1.39), and grade 3 (>1.39) [17].

Standardized CEUS Examination

Standardized US and CEUS were performed for each index nodule according to the established protocol [18, 19]. Different ultrasound instruments were utilized in various centers, complying with recommended CEUS parameters from corresponding manufacturers. Harmonic imaging and a low mechanical index were used for CEUS examinations. A bolus injection of 1.0–2.4 mL of SonoVue (Bracco S.p.A., Milan, Italy) in the antecubital vein followed by a 5-mL saline flush was administered. The CEUS cine loops were observed continuously for at least 60 s after injection; thereafter, the lesions were intermittently imaged every 30 s for 5 min, or until microbubbles had completely washed out from the index lesion. All imaging data were stored in DICOM format.

CEUS LI-RADS Category Assignment

The LI-RADS categories were assigned on the grounds of the latest CEUS LI-RADS scheme released by the American College of Radiology (ACR) Working Group, according to the combination of the arterial and venous phase appearances [20]. Arterial phase hyperenhancement is defined as a lesion becoming globally (APHE in whole) or partially hyperechoic but not with rim or globular peripheral distribution (APHE in part) compared to the surrounding parenchyma in the arterial phase. A rim enhancement pattern (not globular peripheral) corresponds to hyperenhancement in the peripheral region in the arterial phase. Enhanced uniformity represents the homogeneity in the microbubble perfusion zone (excluding intratumoral non-enhanced area) during the peak enhancement period. Necrosis in the tumor demonstrates intratumoral non-enhanced area throughout the entire perfusion period. The feeding artery is defined as a hypertrophic artery directed toward the lesion in the arterial phase, while the intratumoral artery is defined as a thick, linear vasculature pattern inside the lesion in the arterial phase. "Washout" corresponds to the visually assessed reduction in nodule enhancement, in whole or in part, compared to the surrounding parenchyma in the portal venous or late phase. When such washout occurred, it would be further classified into different grades according to its timing, generally as "early" if washout appeared before 60 s following contrast injection or as "late" if it occurred later. In this study, we further subdivided the timing as <45 s, 45–60 s, 60–120 s, >120 s, or no washout. According to the washout intensity, "marked" represents the lesion becoming markedly hypoenhanced or punched out within 2 min; otherwise, it is defined as "mild/moderate" [5, 7, 10, 21]. According to the current version of CEUS LI-RADS, a rim enhancement pattern in the arterial phase (regardless of the venous pattern), or marked and/or early onset venous washout (regardless of the arterial appearance) would be categorized as LR-M. The LR-5 class comprised lesions ≥10 mm with APHE (either global or in part) accompanied by late onset of washout with mild/moderate degree. If the same pattern was observed in lesions <10 mm, the category was LR-4; in addition, lesions ≥2 cm with mild/moderate washout but no APHE or with APHE but no washout of any type would also be categorized as LR-4 [20].

All CEUS clips of lesions were reviewed, and LI-RADS classes were categorized by two experienced radiologists (W.-J.C. and M.H.Y., with more than 9 years of experience in hepatic ultrasound and CEUS) who were blinded to the results of pathologic evaluation and other imaging findings. If there were any discordant findings, the two reviewers were required to discuss the results to reach a consensus. Expert arbitration was performed by a third expert (J.Y., with 15 years of experience in hepatic ultrasound and CEUS) if there was any disagreement in the previous discussion.

Potential Modification of CEUS LI-RADS Category

To explore feasible strategies to improve the sensitivity and accuracy of CEUS LI-RADS, we applied a modification of LI-RADS recommended by Zheng et al. [22], namely, LR-M nodules with hyperenhancement in the arterial phase and early (<60 s) but mild to moderate washout at less than 5 min were reclassified as LR-5.

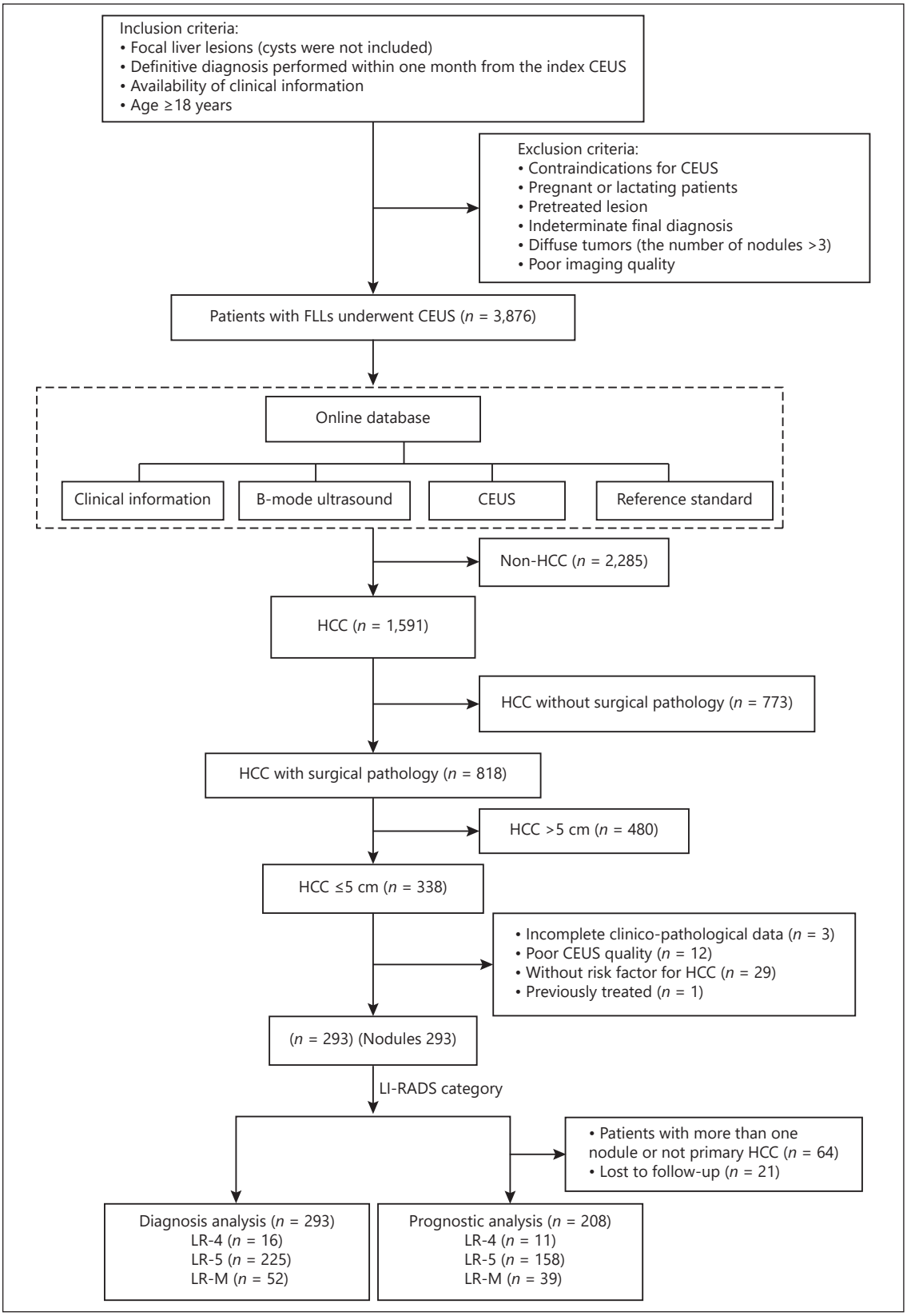

Fig. 1. Flowchart of patient enrollment process.

Table 1. Baseline characteristics patients and tumor characteristics

Variable %	Total (*n* = 293)	LI-RADS categories			*p* value
		LR-4 (*n* = 16)	LR-5 (*n* = 225)	LR-M (*n* = 52)	
Age, years					
<60	197 (67.2)	11 (68.8)	149 (66.2)	37 (71.2)	0.78
≥60	96 (32.8)	5 (31.2)	76 (33.8)	15 (28.8)	
Gender					
Male	249 (85.0)	12 (75.0)	189 (84.0)	48 (92.3)	0.16
Female	44 (15.0)	4 (25.0)	36 (16.0)	4 (7.7)	
Etiology					
HBV	277 (94.5)	15 (93.8)	210 (93.3)	52 (100.0)	0.16
Others[a]	16 (5.5)	1 (6.2)	15 (6.7)	0 (0.0)	
Primary of HCC					
Yes	269 (91.8)	14 (87.5)	204 (90.7)	51 (98.1)	0.17
No	24 (8.2)	2 (12.5)	21 (9.3)	1 (1.9)	
Child-Pugh classification					
A	88 (30.0)	6 (37.5)	68 (30.2)	14 (26.9)	0.72
B	205 (70.0)	10 (62.5)	157 (69.8)	38 (73.1)	
BCLC stage					
0	26 (8.9)	3 (18.8)	21 (9.3)	2 (3.8)	0.27
A	216 (73.7)	9 (56.2)	168 (74.7)	39 (75.0)	
B	51 (17.4)	4 (25.0)	36 (16.0)	11 (21.2)	
Tumor size	3.3±1.0	2.9±1.2	3.2±1.0	3.4±0.9	0.154
≤2 cm	40 (13.7)	4 (25.0)	33 (14.7)	3 (5.8)	
>2 cm, ≤5 cm	253 (86.3)	12 (75.0)	192 (85.3)	49 (94.2)	
HCC differentiation					
Poor	45 (15.4)	1 (6.3)	27 (12.0)	17 (32.7)	<0.001
Moderate	202 (68.9)	9 (56.2)	164 (72.9)	29 (55.8)	
Well	46 (15.7)	6 (37.5)	34 (15.1)	6 (11.5)	
MVI					
+	72 (24.6)	3 (18.8)	55 (24.4)	14 (26.9)	0.80
–	221 (75.4)	13 (81.2)	170 (75.6)	38 (73.1)	
Ki-67[b]	0.20 (0.10–0.30)	0.11 (0.08–0.23)	0.20 (0.10–0.30)	0.30 (0.16–0.48)	0.01
ALT, IU/L[c]	32.0 (21.0–51.0)	31.2 (24.1–58.5)	30.0 (19.9–49.0)	35.5 (27.5–61.6)	0.01
AST, IU/L[c]	31.0 (23.7–44.0)	38.5 (30.0–67.0)	29.1 (23.0–43.0)	32.5 (24.0–50.4)	0.18
Total bilirubin, mg/dL					
≤35	282 (96.2)	16 (100.0)	217 (96.4)	49 (94.2)	0.54
>35	11 (3.8)	0 (0.0)	8 (3.6)	3 (5.8)	
Albumin, mg/mL					
≤38	125 (42.7)	8 (50.0)	94 (41.8)	23 (44.2)	0.79
>38	168 (57.3)	8 (50.0)	131 (58.2)	29 (55.8)	
ALBI grade*					
1	147 (50.2)	8 (50.0)	117 (52.0)	22 (42.3)	0.62
2	119 (40.6)	7 (43.8)	86 (38.2)	26 (50.0)	
3	27 (9.2)	1 (6.2)	22 (9.8)	4 (7.7)	
AFP, ng/mL					
≤20	130 (44.4)	7 (43.8)	103 (45.8)	20 (38.5)	0.73
>20, <100	46 (15.7)	2 (12.5)	37 (16.4)	7 (13.5)	
≥100	117 (39.9)	7 (43.8)	85 (37.8)	25 (48.1)	

Unless otherwise indicated, data are the numerator/denominator of patients and data in parentheses are percentages. ALT, alanine transaminase; AST, aspartate transaminase; BCLC, Barcelona Clinic Liver Cancer; HCC, hepatocellular carcinoma; AFP, alpha-fetoprotein. [a]Others included liver cirrhosis caused by HCV, alcoholic liver disease, or unknown etiology. [b]Ki-67 is the number of immunohistochemistry-positive cells (Ki-67)/total number of cells observed*(100/100), data are median value and data in parenthesis are interquartile range. [c]Data are median value and data in parenthesis is interquartile range.

Table 2. Imaging features among different CEUS LI-RADS categories

Variable	LI-RADS categories				
	all (*n* = 293)	LR-4 (*n* = 16)	LR-5 (*n* = 225)	LR-M (*n* = 52)	*p* value
CEUS					
Enhancement patterns of arterial phase					
APHE in whole	242 (82.6)	9 (56.2)	199 (88.4)	34 (65.4)	<0.001
APHE in part	38 (13.0)	1 (6.3)	26 (11.6)	11 (21.2)	
Iso-enhancement	8 (2.0)	6 (37.5)	0	0	
Rim APHE	7 (2.4)	0	0	7 (13.4)	
Enhanced uniformity					
Yes	235 (80.2)	13 (81.2)	189 (84.0)	33 (63.5)	0.004
No	58 (19.8)	3 (18.8)	36 (16.0)	19 (36.5)	
Necrosis in tumor					
Yes	35 (11.9)	1 (6.2)	20 (8.9)	14 (26.9)	0.001
No	258 (88.1)	15 (93.8)	205 (91.1)	38 (73.1)	
Feeding artery					
Yes	260 (88.7)	12 (75.0)	200 (88.9)	48 (92.3)	0.158
No	33 (11.3)	4 (25.0)	25 (11.1)	4 (7.7)	
Intratumoral artery					
Yes	104 (35.5)	6 (37.5)	79 (35.1)	19 (36.5)	0.967
No	189 (64.5)	10 (62.5)	146 (64.9)	33 (63.5)	
Onset of washout					
<45 s	10 (3.4)	0	0	10 (19.2)	<0.001
45–60 s	40 (13.7)	0	0	40 (76.9)	
60–120 s	151 (51.5)	5 (31.3)	144 (64.0)	2 (3.9)	
>120 s	82 (28.0)	1 (6.2)	81 (36.0)	0	
No washout	10 (3.4)	10 (62.5)	0	0	
Degree of washout					
Mild/moderate	266 (94.0)	6 (100)	225 (100)	35 (67.3)	<0.001
Marked	17 (6.0)	0	0	17 (32.7)	
B-mode					
Echogenicity					
Hypo-	107 (36.5)	6 (37.5)	87 (38.7)	14 (26.9)	0.212
Iso-	67 (22.9)	5 (31.3)	54 (24.0)	8 (15.4)	
Hyper-	68 (23.2)	3 (18.7)	47 (20.9)	18 (34.6)	
Mix-	51 (17.4)	2 (12.5)	37 (16.4)	12 (23.1)	
Halo					
Yes	104 (35.5)	4 (25.0)	80 (35.6)	20 (38.5)	0.616
No	189 (64.5)	12 (75.0)	145 (64.4)	32 (61.5)	
Intratumoral vascularity					
Yes	149 (50.9)	4 (25.0)	117 (52.0)	28 (53.8)	0.101
No	144 (49.1)	12 (75.0)	108 (48.0)	24 (46.2)	

Furthermore, we analyzed the specific CEUS patterns of HCC in the LR-M category and varied diagnoses according to current criteria, including the classic pattern for HCC with CEUS (hyperenhancement in the arterial phase followed by washout) [3] and the EASL HCC guideline (hyperenhancement in the arterial phase with late-onset (>60 s) washout of mild intensity) [2].

Histologic and Immunohistochemistry Information

All pathological specimens were fixed with formalin and then embedded in paraffin wax. The diagnosis of pathologic differentiation (well, moderate, or poor according to the WHO histologic grade system) and microvascular invasion were determined by hematoxylin and eosin staining. Immunohistochemistry (IHC) results were analyzed by trained pathologists. The Ki-67-positive cellular index represented the presence of nuclear staining, and all stained nuclei were regarded as positive (regardless of the staining intensity). The percentage of positive cells was calculated by counting 1,000 cells/slide in five randomly selected fields with a conventional light microscope (at ×100 magnification). The computational formula was as follows: Number of IHC-positive cells (Ki-67)/total number of cells observed ×100 [23].

Table 3. Imaging features and biological characteristics of hepatocellular carcinoma

Variable	Differentiation			*p* value	Ki-67[#]	*p* value	MVI (+/–)	*p* value
	poor (*n* = 45)	moderate (*n* = 202)	well (*n* = 46)					
CEUS								
Enhancement patterns of arterial phase								
APHE in whole	35 (77.8)	168 (83.2)	39 (84.8)	0.976	0.25±0.18	0.018*	58/184	0.872
APHE in part	8 (17.8)	25 (12.4)	5 (10.9)		0.30±0.18		11/27	
Iso-enhancement	1 (2.2)	4 (2.0)	1 (2.2)		0.33±0.25		1/5	
Rim APHE	1 (2.2)	5 (2.4)	1 (2.2)		0.53±0.28		2/5	
Enhanced uniformity								
Yes	34 (75.6)	163 (80.7)	38 (82.6)	0.667	0.25±0.17	0.010*	54/181	0.202
No	11 (24.4)	39 (19.3)	8 (17.4)		0.33±0.23		18/40	
Necrosis in tumor								
Yes	7 (15.6)	24 (11.9)	4 (8.7)	0.600	0.37±0.21	0.007*	9/26	0.867
No	38 (84.4)	178 (88.1)	42 (91.3)		0.25±0.18		63/195	
Feeding artery								
Yes	39 (86.7)	181 (89.6)	40 (87.0)	0.782	0.26±0.19	0.749	63/197	0.702
No	6 (13.3)	21 (10.4)	6 (13.0)		0.25±0.21		9/24	
Intratumoral artery								
Yes	14 (31.1)	75 (37.1)	15 (32.6)	0.677	0.27±0.19	0.676	27/77	0.682
No	31 (68.9)	127 (62.9)	31 (67.4)		0.26±0.19		45/144	
Onset of washout								
<45 s	3 (6.7)	6 (3.0)	1 (2.1)	<0.001*	0.39±0.27	0.007*	2/8	0.879
45–60 s	14 (31.1)	21 (10.4)	5 (10.9)		0.32±0.20		12/28	
60–120 s	26 (57.8)	103 (51.0)	22 (47.8)		0.27±0.19		38/113	
>120 s	2 (4.4)	67 (33.2)	13 (28.3)		0.22±0.15		18/64	
No washout	0	5 (2.4)	5 (10.9)		0.11±0.06		2/8	
Degree of washout								
Mild/moderate	40 (88.9)	186 (94.4)	40 (97.6)	0.216	0.26±0.18	0.017*	63/203	0.143
Marked	5 (11.1)	11 (5.6)	1 (2.4)		0.41±0.29		7/10	
B-mode								
Echogenicity								
Hypo-	16 (35.6)	74 (36.6)	17 (36.9)	0.996	0.27±0.18	0.564	23/84	0.585
Iso-	11 (24.4)	45 (22.3)	11 (23.9)		0.27±0.21		19/48	
Hyper-	11 (24.4)	48 (23.8)	9 (19.6)		0.23±0.16		15/53	
Mix-	7 (15.6)	35 (17.3)	9 (19.6)		0.28±0.21		15/36	
Halo								
Yes	16 (35.6)	70 (34.7)	18 (39.1)	0.849	0.25±0.20	0.434	23/81	0.468
No	29 (64.4)	132 (65.3)	28 (60.9)		0.27±0.18		49/140	
Intratumoral vascularity								
Yes	27 (60.0)	101 (50.0)	21 (45.7)	0.356	0.27±0.19	0.989	36/113	0.868
No	18 (40.0)	101 (50.0)	25 (54.3)		0.26±0.18		36/108	

[#] Ki-67 is the number of immunohistochemistry-positive cells (Ki-67)/total number of cells observed* (100/100); data presented in this table were mean ± SD.

Follow-Up

After tumor resection, all patients were followed up according to institutional practice, including abdomen-pelvis ultrasound or contrast-enhanced CT/MRI and laboratory tests (including serum alpha-fetoprotein [AFP]) 1 month after initial treatment and every four to 6 months thereafter. The endpoint of this study was RFS, which was defined as the time from the date of curative surgery to the time of any recurrence or death. Intrahepatic recurrence was defined as the development of new tumors within the liver, including local recurrence, which was defined as any recurrence abutting the treatment site, and distant recurrence, defined as recurrence without contact with the resection margin [24, 25]. Extrahepatic recurrence was determined by chest CT, brain MRI, whole-body bone scintigraphy, or other necessary modalities. Patients were followed until recurrence, death, or the end date of this study (March 15, 2022). Follow-up information was collected and reviewed from patients' medical records in each center, which should be simultaneously sent to the sponsor of this study to summarize and recheck.

For patients who stopped attending the hospitals, information on the living status, time of death, or cause of death was confirmed by telephone interview through the reserved phone number of the patient's families.

Statistical Analysis

Statistical analysis was performed using SPSS (Version 23; IBM, Armonk, NY, USA, and MedCalc, Ostend, Belgium). Continuous variables with normal distribution were reported as the mean ± SD. Data with skewed distributions were presented as the median and range. Differences between numerical variables were analyzed by parametric (*t* test) or nonparametric tests (the Mann-Whitney test) according to the distribution type of the variables. Qualitative variables were presented as numbers and percentages and analyzed by χ^2 test or Fisher's exact test. Correlation analyses were performed using Kendall's correlation method. Missing values were imputed using multiple methods. The RFS rate was estimated by the Kaplan-Meier method with the log-rank test. To determine whether LI-RADS category influenced the RFS, we performed different analytical strategies. First, we conducted analyses between LI-RADS classes and RFS from multivariable Cox analysis with and without additional adjustment for potential prognostic factors. Furthermore, univariate and multivariate analyses of all data were performed using the Cox proportional hazards regression model for RFS. In addition, we compare the RFS between the patients with modified LR-5 (originally LR-M) nodules and those with modified LR-M nodules (consistently LR-M). The variables with $p < 0.1$ in univariate analysis or some potential risk factors were included in the final multivariate model. A two-sided p value less than 0.05 was considered statistically significant.

Results

Patient Characteristics

Based on the selection criteria, a total of 293 patients (mean age, 53.5 ± 10.9 years; range 27–83 years) with 293 HCCs (mean size ± standard deviation: 3.3 ± 1.0 cm, range: 1.2–5.0 cm) from 20 centers were included (online suppl. Table S1; for all online suppl. material, see www.karger.com/doi/10.1159/000527498). The clinical characteristics of the patients and biological characteristics are summarized in Table 1. On the basis of the major imaging features, 16 nodules were assigned as LR-4, 225 nodules were LR-5, and 52 nodules were LR-M.

Imaging Features among CEUS LI-RADS Categories

All HCC cases were categorized into LR-4 (16/293), LR-5 (225/293), or LR-M (52/293). No significant differences were found among all three CEUS LI-RADS categories of HCCs in echogenicity, presence of halo and intratumoral vascularity of B-mode imaging features, and feeding artery and intratumoral artery of CEUS imaging features ($p > 0.05$). However, there were significant differences among the enhancement patterns of the arterial phase, enhanced uniformity, presence of necrosis in the tumor, onset of washout, and degree of washout ($p < 0.05$) (Table 2).

Imaging Features and Biological Characteristics of HCC

The imaging features and various biological characteristics of HCC are summarized in Table 3. Only the onset of washout and differentiation showed a significant difference between differentiation grades: poor differentiation presented a much higher proportion of early washout (6.7% less than 45 s after contrast materials injection and 31.7% between 45 s and 60 s) than moderate and well differentiation (3.0% and 10.4%; 2.1% and 10.9%, respectively) ($p < 0.001$). Kendall's correlation coefficient was calculated ($r = 0.125$; $p < 0.05$). In contrast, other imaging features, such as enhancement patterns of the arterial phase, enhanced uniformity, and presence of necrosis in tumor, showed no significant difference among various differentiation grades ($p > 0.05$).

There were significant differences in the level of Ki-67 in the enhancement patterns of the arterial phase, enhanced uniformity, presence of necrosis in the tumor, onset of washout, and degree of washout ($p < 0.05$), and the correlation coefficients were 0.08 ($p = 0.25$), −0.153 ($p = 0.027$), 0.200 ($p = 0.004$), −0.114 ($p = 0.100$), and −0.093 ($p = 0.187$). However, no significant differences were found between MVI and the above imaging characteristics, either in B-mode or CEUS imaging features ($p > 0.05$).

CEUS LI-RADS Category and Biological Characteristics of HCC

To better understand the reasons why HCC presented different perfusion or washout patterns, we analyzed the biological characteristics of HCC, including differentiation, level of Ki-67 expression and MVI, and CEUS LI-RADS patterns. The results showed that the differentiation

Fig. 2. Imaging features and biological characteristics of HCC categorized as CEUS LR-5 in a 49-year-old woman with chronic HBV infection. **a** Slightly hyperechoic nodule of 41 mm in the segment 6 of the right liver lobe. **b** Hyperenhancement in arterial. **c** Mild washout in the portal phase (109 s). **d** Moderate washout in the late phase (180 s). **e** Hematoxylin-eosin staining showed the well differentiated hepatocellular carcinoma (original magnification ×100). **f** Immunohistochemistry showed that low level of Ki-67 expression (Ki-67+, 15%) (original magnification ×100).

(For figure see next page.)

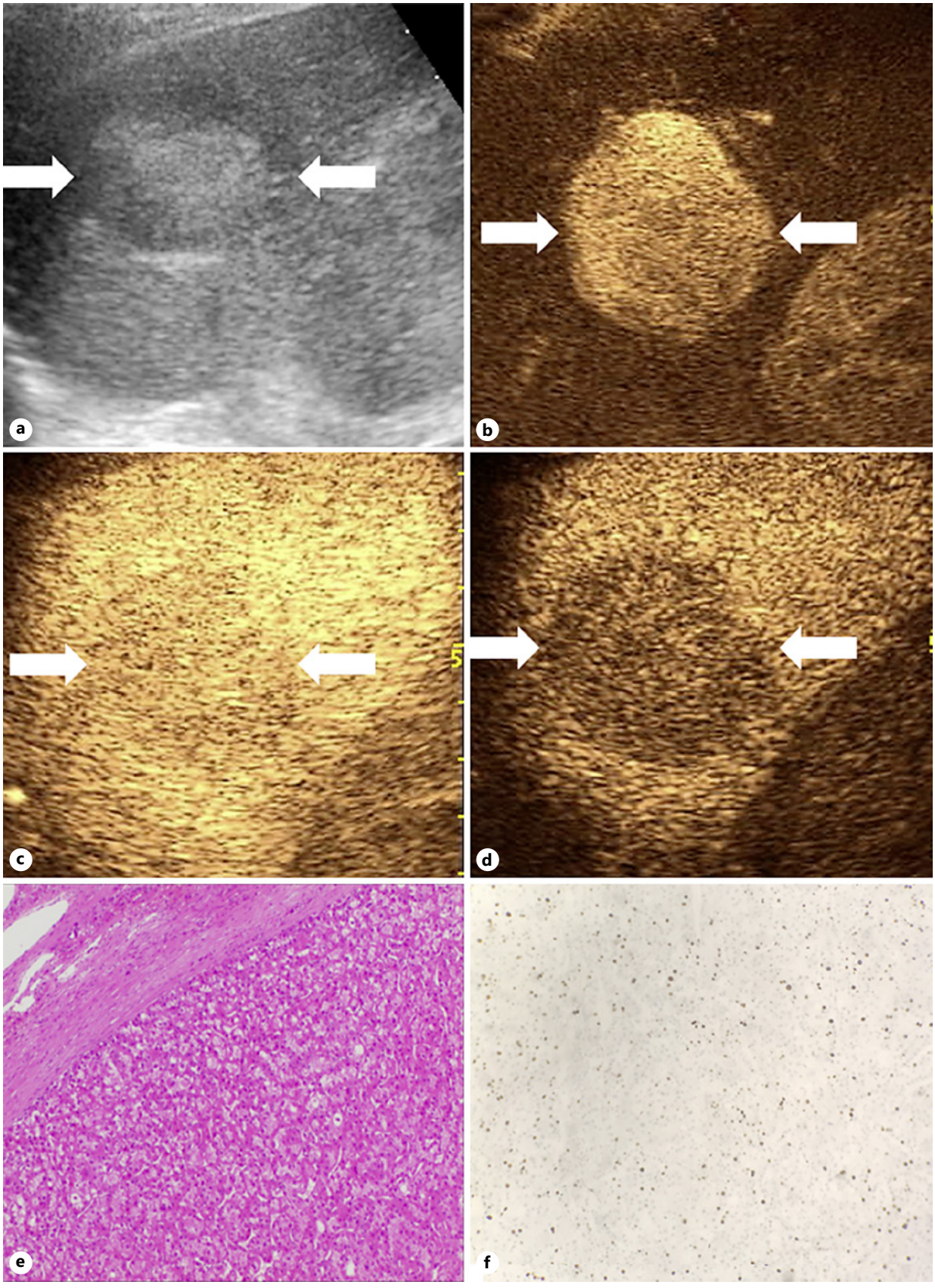

2

and levels of Ki-67 expression were significantly different among the three categories; that is, the percentage of poor differentiation and level of Ki-67 were higher in the LR-M than in the LR-5 and LR-4 categories ($p < 0.05$) (Fig. 2, Fig. 3). The correlation was weak, with a coefficient of 0.229 between LI-RADS and Ki-67 ($p = 0.001$) and a coefficient of 0.176 between LI-RADS and differentiation ($p = 0.002$). However, no significant differences were found between MVI and CEUS LI-RADS categories ($p > 0.05$) (Table 1).

Correlation between LI-RADS Category and Recurrence-Free Survival

Finally, 208 nodules in 208 patients with single and primary HCC were included in the final prognostic analysis (online suppl. Table S2). The median follow-up period was 23.0 months (interquartile range, 15.0–32.7 months). Of the 208 HCC patients, 9 (4.3%) died by the end of the last follow-up (March 15, 2022). The recurrence-free survival rates at 6, 12, 18, and 24 months for the whole study population were 94.3%, 83.8%, 76.7%, and 72.6%, respectively, and there was no difference among the different LI-RADS categories (online suppl. Table S3).

In analyses adjusted for age, gender, and diameter (model 2) and then Ki-67 (model 3), HCC differentiation (model 4), and MVI status (model 5) successively, the RFS showed no significant difference among LR-4, LR-5, and LR-M ($p > 0.05$) (Table 4). In univariate and multivariate survival analyses, only the level of Ki-67 (cutoff value was 30%) was significantly associated with RFS ($p = 0.007$). Specifically, CEUS LI-RADS classes also had no statistical impact on RFS ($p > 0.05$) (online suppl. Table S4).

Stratification analysis of Kaplan-Meier curves of RFS based on LI-RADS classes also did not show a significant difference (Fig. 4). Further subgroup analysis found that patients with a high level of Ki-67 (≥30%) in the LR-5 subgroup ($n = 225$) presented with a worse prognosis than those with a low level (<30%), while in the LR-4 and LR-M subgroups, the level of Ki-67 showed no significant impact on RFS (Fig. 4). Although Kaplan-Meier curves of RFS showed that a high level of Ki-67 was associated with a worse prognosis than a low level in all patients, stratification analysis demonstrated that neither in the high level of Ki-67 subgroup (≥30%) ($n = 101$) nor in the low level subgroup (<30%) ($n = 107$) did LI-RADS categories have a significant impact on RFS ($p > 0.05$) (online suppl. Fig. S1).

In addition, we also performed Kaplan-Meier curves of RFS based on LI-RADS classes in the initial patient cohort. After excluding 21 cases lost to follow-up, 272 cases were ultimately enrolled, including 64 cases with more than one nodule and recurrent HCC, and the results also verified that CEUS LI-RADS classes had no statistical impact on RFS (online suppl. Fig. S2).

Potential Modification of CEUS LI-RADS Category

Since HCC assigned to LR-M did not show worse prognosis than LR-5, we applied a modified LR-M criterion: nodules presenting hyperenhancement in the arterial phase and early (<60 s) but mild to moderate washout at less than 5 min were reclassified as LR-5, and the results showed that up to

Table 4. Association of LI-RADS category with recurrence-free survival

Step group	Hazard ratio (95% CI)									
	Model 1[a]	*p* value	Model 2[b]	*p* value	Model 3[c]	*p* value	Model 4[d]	*p* value	Model 5[e]	*p* value
LR-4	1 [Reference]		1 [Reference]		1 [Reference]		1 [Reference]		1 [Reference]	
LR-5	0.8 (0.3, 2.7)	0.784	0.6 (0.2, 1.9)	0.361	0.5 (0.2, 1.8)	0.301	0.5 (0.2, 1.8)	0.323	0.5 (0.2, 1.9)	0.329
LR-M	0.7 (0.2, 2.5)	0.571	0.4 (0.1, 1.7)	0.231	0.3 (0.1, 1.2)	0.099	0.3 (0.1, 1.2)	0.099	0.3 (0.1, 1.2)	0.099

[a] No adjusted. [b] Adjusted for age, gender, and diameter. [c] Adjusted for variables included in model 2 + ki-67. [d] Adjusted for variables included in model 3 + differentiation. [e] Adjusted for variables included in model 4 + MVI.

Fig. 3. Imaging features and biological characteristics of HCC categorized as CEUS LR-M in a 64-year-old man with chronic HBV infection. **a** Slightly hypoechoic nodule of 45 mm in the segment 8 of the right liver lobe. **b** Partial hyperenhancement in arterial. **c** Early washout in the portal phase (50 s). **d** Marked washout in the portal phase (75 s). **e** Hematoxylin-eosin staining showed the poor differentiated hepatocellular carcinoma (original magnification ×100). **f** Immunohistochemistry showed that high level of Ki-67 expression (Ki-67+, 80%) (original magnification ×100).

(For figure see next page.)

67.3% (35/52) of HCC nodules in the current LR-M classes could be correctly assigned to LR-5. According to the classic pattern for HCC with CEUS (hyperenhancement in the arterial phase followed by washout), 86.5% (45/52) of nodules in the LR-M category in this study were recognized as HCC. While the EASL guideline was not helpful in

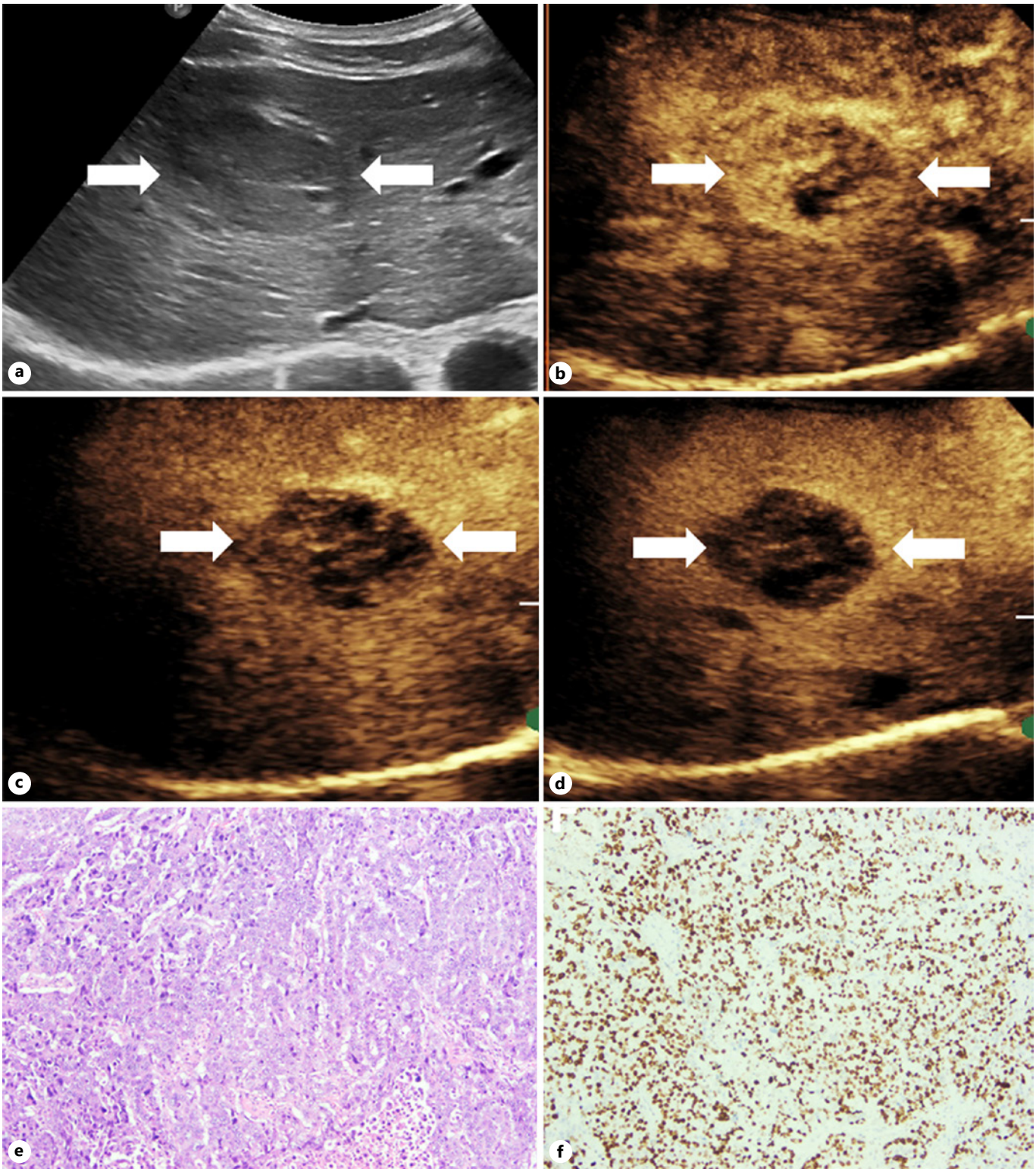

3

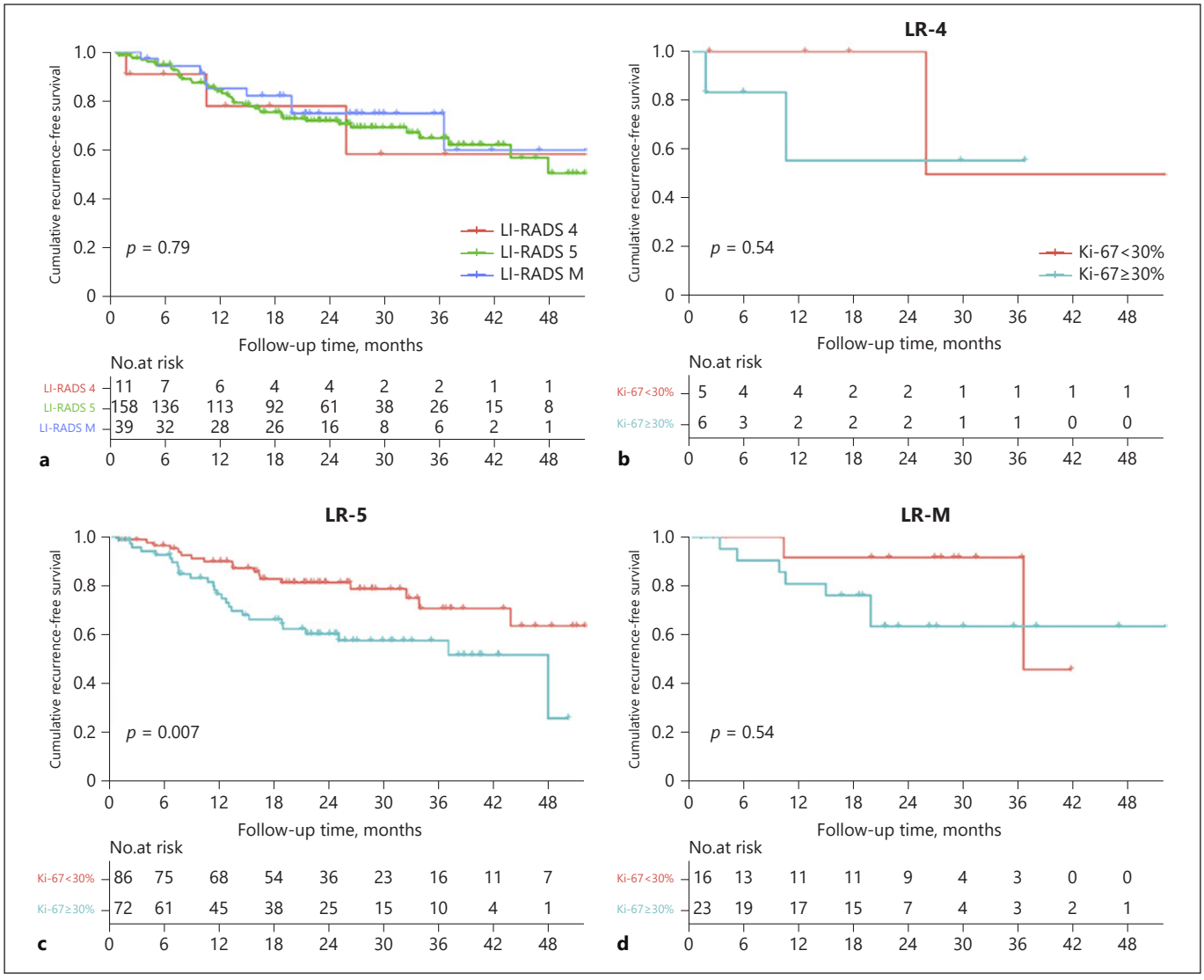

Fig. 4. Kaplan-Meier curves of recurrence-free survival (RFS) among different LI-RADS categories in 208 single and primary HCC patients. **a** Total patients. **b–d** Stratification analysis of according to level of Ki-67 in LR-4 (**b**), LR-5 (**c**), and LR-M (**d**). The short vertical lines indicate censored data.

improving the diagnostic ability for HCC in LR-M (online suppl. Table S5), RFS between the patients with modified LR-5 (originally LR-M) nodules (n = 27) and those with modified LR-M nodules (consistently LR-M) (n = 12) showed no significant difference (online suppl. Fig. S3).

Discussion

In this study, we showed that the CEUS LI-RADS category determined mainly by major CEUS imaging features can be impacted by some biological characteristics of HCC, including differentiation and levels of Ki-67 expression. Poor differentiation and high levels of Ki-67 were more frequently classified into the LR-M category, whereas well differentiation and low levels of Ki-67 were more frequently classified into the LR-4 category. Our findings further indicate that patients with HCC ≤5 cm in different CEUS LI-RADS classes have no significant differences in RFS after resection.

Differentiation, an important biological characteristic of HCC, has been proven to be associated with several major CEUS imaging features, especially washout, and would no doubt impact the CEUS LI-RADS category.

Several studies indicated that moderately differentiated HCCs generally showed classic enhancement features, including hypervascularity in the arterial phase with dysmorphic arteries (up to 96% proportion) and typical late washout (90–300 s) [12]. Poorly differentiated HCCs exhibited much earlier washout, and HCCs with well differentiation manifested as washout in the delayed phase or no washout (41.9% and 21.5%, respectively) [11, 12, 26]. A possible explanation may be multistep hepatocarcinogenesis for HCC: as the tumor progresses, the arterial flow from newly formed tumor vessels (neoangiogenesis) progressively increases and gradually replaces normal arterial and portal blood flow [27–29]. However, to our knowledge, few studies have evaluated correlations between tumor differentiation of HCC and the CEUS LI-RADS category [30]. Chen et al. [30] reported that histological grade influenced CEUS LR-5 and LR-TIV categories, and low-grade HCCs occurred more frequently in the LR-5 category whereas high-grade HCCs occurred more frequently in the LR-TIV category; regardless, they alleged that HCC histological grade exhibited limited impact on CEUS LI-RADS. In this study, the results based on prospective, multicenter data with histologic diagnosis by resection revealed that the onset of washout showed a significant difference between differentiation grades and that poor differentiation presented with a much higher proportion of early washout (<60 s), while moderate and well differentiation were more frequently presented with late or no washout ($p \leq 0.001$). Therefore, a significant difference was found in the CEUS LI-RADS category of HCCs in differentiation, and poor differentiation was more frequently classified into the LR-M category, whereas well differentiation was more frequently classified into the LR-4 category. The discrepancies between this study and Cheng et al.'s findings were possibly due to different populations of enrolled subjects across the studies, and further studies are still needed for verification.

Ki-67, a biological characteristic of HCC that is often considered a marker of cellular proliferation [31–33], also shows association with several major CEUS imaging features and ultimately impacts the CEUS LI-RADS category. HCCs with high levels of Ki-67 expression tend to grow heterogeneously, where tumor cell and vessel density is inhomogeneous. Nakamura et al. revealed that the proportion of Ki-67-positive cells was significantly higher in HCC nodules with irregular vascular patterns on CEUS [13], and a similar correlation has also been verified in MRI of HCC [14]. In this study, we also found that higher expression of Ki-67 corresponds to more frequent features with irregular perfusion in the arterial phase, such as rim APHE, heterogeneity in tumor and necrosis in tumor, and much earlier onset of washout and greater degree of washout. Eventually, HCC nodules with much higher levels of Ki-67 expression were more frequently categorized into the LR-M category, while those with lower levels of Ki-67 were more frequently classified into the LR-4 category.

However, MVI status, another important biological characteristic of HCC, showed no association with the CEUS LI-RADS category in this study. The interpretation may be that the major imaging features used to define LI-RADS have little correlation with MVI status. Although some studies reported that imaging features such as non-smooth tumor margins, arterial peritumoral enhancement, irregular circular enhancement, or radiological characteristics of the capsule might be associated with MVI in some studies, the findings varied [15, 34, 35]. Interestingly, studies suggested that CEUS-based radiomics showed a favorable prediction value for MVI in HCC patients preoperatively [36], implying that high-throughput data mining of CEUS rather than subjective judgment by the radiologist is more likely to provide a promising evaluation of MVI, which is worthy of further investigation.

We further evaluated the correlation between the CEUS LI-RADS category and RFS of HCC patients after radical resection; however, no significant correlation was found, either using univariate and multivariate analysis or extended Cox models using LI-RADS categories with and without additional adjustment for other risk factors. That is, HCC nodules assigned in LR-4 have no better clinical outcome than typical HCC (LR-5), while LR-M has no worse outcome than typical HCC. The results that RFS was similar between HCCs with LR-4 and LR-5 patterns were consistent with previous studies [25, 37] and had also been confirmed by CT/MRI LI-RADS classes [37, 38]. However, when referred to LR-M, no consistent findings have been reported. Although some MRI imaging studies implied that lesions categorized as LR-M showed significantly worse disease-free survival than lesions categorized as LR-3/4/5, lesions classified in LR-M patterns in their study included intrahepatic cholangiocarcinoma (ICC) and biphenotypic carcinomas [39]. Therefore, the possible interpretation may be that tumors in "real" LR-M (malignant but not HCC) usually correspond to ICC, metastasis, or other more aggressive malignant tumors, which result in worse prognosis rather than HCC "misclassified" in the LR-M class [37, 39, 40]. The results of this study indicate that HCCs classified as CEUS LR-M have no worse prognosis than those classified as LR-5 and LR-4. In addition, although our study found that the level of Ki-67 was a significant predictor of RFS ($p = 0.007$), further

subgroup analysis demonstrated that, only in the LR-5 subgroup, cases with a high-level Ki-67 (≥30%) presented with a worse prognosis than low-level cases (<30%). No differences were found in the LR-4 and LR-M subgroups, and neither in the high-level Ki-67 subgroup (≥30%) nor in the low-level subgroup (<30%) did LI-RADS categories have a statistical impact on RFS ($p > 0.05$) (online suppl. Fig. S1). The interpretation may be that the correlation between LI-RADS and Ki-67 was weak ($r = 0.229$) ($p = 0.001$), and differences in Ki-67 levels among various LI-RADS categories were not significant enough.

However, the results that HCCs in different CEUS LI-RADS classes have no significant differences in RFS after resection might negatively affect liver lesion management. In the current CEUS LI-RADS version, the LR-4 nodule is defined as probably having HCC, which may receive nonsurgical treatments or imaging follow-up, while for LR-M, more aggressive intervention may be applied [5]. To reduce the potential risk of HCC underdiagnosis and progression or overdiagnosis and overtreatment, further evaluations (especially biopsy) should be considered to obtain histological proof [2, 5]. However, these strategies might raise novel concerns about increasing biopsy and the consequent risk of complications and increasing cost, so the realistic consideration may be aimed at improving diagnostic efficacy of LI-RADS. Zheng et al. [22] advocated a modification of LI-RADS such that category LR-M nodules with arterial phase hyperenhancement and early washout but not punched-out should be reclassified into LR-5, which would obtain an increased specificity and PPV of LR-M as a predictor of non-HCC malignancy while increasing the sensitivity of LR-5 and doing little to weaken specificity and PPV. In our study, we also verified those findings; that is, nearly 67.3% of HCC (35/52) in the LR-M category presented with hyperenhancement in the arterial phase and early (<60 s) but mild to moderate washout at less than 5 min. In addition, according to the classic pattern for HCC with CEUS (hyperenhancement in the arterial phase followed by washout), 86.5% (45/52) of nodules in the LR-M category in this study would be correctly recognized as HCC; however, this pattern had been proved to be with high potential risk of misdiagnosis in ICC [41]. Thus, reclassification of those cases into LR-5 would potentially improve the diagnostic efficacy of CEUS for HCC. Furthermore, our results indicate that RFS between the patients with modified LR-5 (originally LR-M) nodules and those with LR-M nodules consistently showed no significant difference. Therefore, the take-home message is that downgrading those lesions from LR-M classes to LR-5 may avoid much more unnecessarily expensive and invasive methods to further confirm without negatively affecting prognosis.

There were several limitations in this study. First, our study sample was predominantly composed of HCC patients with chronic hepatitis B infection. Therefore, the present findings may not be immediately applied to patients with other etiologic causes. Second, to collect more accurate and abundant histologic information while eliminating interference mainly accompanied by a larger diameter (such as a significant risk of MVI or necrosis in the tumor, etc.), we only included HCC lesions that received surgery with diameters no more than 5 cm, which may cause potential bias. Third, the follow-up time was relatively short (median follow-up, 23 months) in this study; thus, further studies with much longer follow-up are needed to verify whether the long-term prognosis of HCC nodules still shows no difference among different LI-RADS classes. Fourth, interobserver variability evaluation (reader agreement) was not performed for CEUS LI-RADS categorization in this study.

In conclusion, the biological characteristics of HCC, including tumor differentiation and Ki-67 level, impacted the CEUS LI-RADS classification, that poor differentiation and high levels of Ki-67 were more frequently classified into the LR-M category, whereas well differentiation and low levels of Ki-67 were more frequently classified into the LR-4 category. However, HCCs assigned to different CEUS LI-RADS classes showed no significant differences in RFS after resection.

Acknowledgments

We thank all centers that participated in this study for their hard work and full cooperation.

Statement of Ethics

The prospectively multicenter study was reviewed and approved by the Ethical Committee of Chinese PLA general hospital (S2017-046-03) as the coordinating center; based on this, all other clinical partners received ethical approval for the study. Retrospective analysis based on the collected data in this study had been approved by each center and was in line with the Declaration of Helsinki. Written informed consent was obtained from participants in this study.

Conflict of Interest Statement

The authors have no conflicts of interest to declare.

Funding Sources

This work was supported by Grants 81971625, 91859201, 82102076, and 82030047 from the National Natural Science Foundation of China. The funders had no role in study design, data collection and analysis, decision to publish, or preparation of the manuscript.

Author Contributions

Wen-Jia Cai, Jie Yu, and Ping Liang: full access to all of the data in the study, responsible for the integrity and the accuracy of the data analysis, study conception and design, and manuscript drafting. Minghua Ying, Rong-Qin Zheng, Jintang Liao, Baoming Luo, Lina Tang, Wen Cheng, Hong Yang, An Wei, Yilin Yang, Hui Wang, Yan-Chun Luo, Cun Liu, Hui Zhong, and Qi Yang: data collection. Wen-Jia Cai, Minghua Ying, and Yan-Chun Luo: data analysis. All authors: final approval of the manuscript.

Data Availability Statement

All data generated or analyzed during this study are included in this article and its online supplementary material file. Further inquiries can be directed to the corresponding author.

References

1 Roberts LR, Sirlin CB, Zaiem F, Almasri J, Prokop LJ, Heimbach JK, et al. Imaging for the diagnosis of hepatocellular carcinoma: a systematic review and meta-analysis. Hepatology. 2018 Jan;67(1):401–21.
2 European Association for the Study of the Liver Electronic address easloffice@easloffliceeuEuropean Association for the Study of the Liver. EASL clinical practice guidelines: management of hepatocellular carcinoma. J Hepatol. 2018 Jul;69(1):182–236.
3 Dietrich CF, Nolsøe CP, Barr RG, Berzigotti A, Burns PN, Cantisani V, et al. Guidelines and good clinical practice recommendations for contrast enhanced ultrasound (CEUS) in the liver: update 2020 – WFUMB in cooperation with EFSUMB, AFSUMB, AIUM, and FLAUS. Ultraschall Med. 2020 Oct;41(5):562–85.
4 Kim TH, Kim SY, Tang A, Lee JM. Comparison of international guidelines for noninvasive diagnosis of hepatocellular carcinoma: 2018 update. Clin Mol Hepatol. 2019 Sep;25(3):245–63.
5 Quaia E. State of the art: LI-RADS for contrast-enhanced US. Radiology. 2019 Oct;293(1):4–14.
6 Wilson SR, Lyshchik A, Piscaglia F, Cosgrove D, Jang HJ, Sirlin C, et al. Ceus li-rads: algorithm, implementation, and key differences from CT/MRI. Abdom Radiol. 2018 Jan;43(1):127–42.
7 Terzi E, Iavarone M, Pompili M, Veronese L, Cabibbo G, Fraquelli M, et al. Contrast ultrasound LI-RADS LR-5 identifies hepatocellular carcinoma in cirrhosis in a multicenter restropective study of 1,006 nodules. J Hepatol. 2018 Mar;68(3):485–92.
8 Zhou H, Zhang C, Du L, Jiang J, Zhao Q, Sun J, et al. Contrast-enhanced ultrasound liver imaging reporting and data system in diagnosing hepatocellular carcinoma: diagnostic performance and interobserver agreement. Ultraschall Med. 2022 Feb;43(1):64–71.
9 Schellhaas B, Bernatik T, Bohle W, Borowitzka F, Chang J, Dietrich CF, et al. Contrast-enhanced ultrasound algorithms (CEUS-LIRADS/ESCULAP) for the noninvasive diagnosis of hepatocellular carcinoma: a prospective multicenter DEGUM study. Ultraschall Med. 2021 Apr;42(2):e20–86.
10 Lyshchik A, Kono Y, Dietrich CF, Jang HJ, Kim TK, Piscaglia F, et al. Contrast-enhanced ultrasound of the liver: technical and lexicon recommendations from the ACR CEUS LI-RADS working group. Abdom Radiol. 2018 Apr;43(4):861–79.
11 Feng Y, Qin XC, Luo Y, Li YZ, Zhou X. Efficacy of contrast-enhanced ultrasound washout rate in predicting hepatocellular carcinoma differentiation. Ultrasound Med Biol. 2015 Jun;41(6):1553–60.
12 Jang HJ, Kim TK, Burns PN, Wilson SR. Enhancement patterns of hepatocellular carcinoma at contrast-enhanced US: comparison with histologic differentiation. Radiology. 2007 Sep;244(3):898–906.
13 Nakamura I, Hatano E, Tada M, Kawabata Y, Tamagawa S, Kurimoto A, et al. Enhanced patterns on intraoperative contrast-enhanced ultrasonography predict outcomes after curative liver resection in patients with hepatocellular carcinoma. Surg Today. 2021 May;51(5):764–76.
14 Li Y, Chen J, Weng S, Sun H, Yan C, Xu X, et al. Small hepatocellular carcinoma: using MRI to predict histological grade and Ki-67 expression. Clin Radiol. 2019 Aug;74(8):653.e1–e9.
15 Zhang D, Wei Q, Wu GG, Zhang XY, Lu WW, Lv WZ, et al. Preoperative prediction of microvascular invasion in patients with hepatocellular carcinoma based on radiomics nomogram using contrast-enhanced ultrasound. Front Oncol. 2021;11:709339.
16 Lee S, Kim SH, Lee JE, Sinn DH, Park CK. Preoperative gadoxetic acid-enhanced MRI for predicting microvascular invasion in patients with single hepatocellular carcinoma. J Hepatol. 2017 Sep;67(3):526–34.
17 Chan AWH, Zhong J, Berhane S, Toyoda H, Cucchetti A, Shi K, et al. Development of pre and post-operative models to predict early recurrence of hepatocellular carcinoma after surgical resection. J Hepatol. 2018 Dec;69(6):1284–93.
18 Yang Q, Wei J, Hao X, Kong D, Yu X, Jiang T, et al. Improving B-mode ultrasound diagnostic performance for focal liver lesions using deep learning: a multicentre study. EBioMedicine. 2020 Jun;56:102777.
19 Claudon M, Dietrich CF, Choi BI, Cosgrove DO, Kudo M, Nolsøe CP, et al. Guidelines and good clinical practice recommendations for contrast enhanced ultrasound (CEUS) in the liver: update 2012 – a WFUMB-EFSUMB initiative in cooperation with representatives of AFSUMB, AIUM, ASUM, FLAUS and ICUS. Ultraschall Med. 2013 Feb;34(1):11–29.
20 Kono Y, Lyshchik A, Cosgrove D, Dietrich CF, Jang HJ, Kim TK, et al. Contrast enhanced ultrasound (CEUS) liver imaging reporting and data system (LI-RADS®): the official version by the American College of Radiology (ACR). Ultraschall Med. 2017 Jan;38(1):85–6.
21 Sato K, Tanaka S, Mitsunori Y, Mogushi K, Yasen M, Aihara A, et al. Contrast-enhanced intraoperative ultrasonography for vascular imaging of hepatocellular carcinoma: clinical and biological significance. Hepatology. 2013 Apr;57(4):1436–47.
22 Zheng W, Li Q, Zou XB, Wang JW, Han F, Li F, et al. Evaluation of contrast-enhanced US LI-RADS version 2017: application on 2020 liver nodules in patients with hepatitis B infection. Radiology. 2020 Feb;294(2):299–307.
23 Li HH, Qi LN, Ma L, Chen ZS, Xiang BD, Li LQ. Effect of KI-67 positive cellular index on prognosis after hepatectomy in Barcelona Clinic Liver Cancer stage A and B hepatocellular carcinoma with microvascular invasion. Onco Targets Ther. 2018;11:4747–54.
24 Mohkam K, Dumont PN, Manichon AF, Jouvet JC, Boussel L, Merle P, et al. No-touch multibipolar radiofrequency ablation vs. surgical resection for solitary hepatocellular carcinoma ranging from 2 to 5 cm. J Hepatol. 2018 Jun;68(6):1172–80.
25 Choi SH, Byun JH, Lim YS, Lee SJ, Kim SY, Won HJ, et al. Liver imaging reporting and data system: patient outcomes for category 4 and 5 nodules. Radiology. 2018 May;287(2):515–24.

26 Yang D, Li R, Zhang XH, Tang CL, Ma KS, Guo DY, et al. Perfusion characteristics of hepatocellular carcinoma at contrast-enhanced ultrasound: influence of the cellular differentiation, the tumor size and the underlying hepatic condition. Sci Rep. 2018 Mar 16;8(1):4713.
27 Di Tommaso L, Sangiovanni A, Borzio M, Park YN, Farinati F, Roncalli M. Advanced precancerous lesions in the liver. Best Pract Res Clin Gastroenterol. 2013 Apr;27(2):269–84.
28 International Consensus Group for Hepatocellular NeoplasiaThe International Consensus Group for Hepatocellular Neoplasia. Pathologic diagnosis of early hepatocellular carcinoma: a report of the international consensus group for hepatocellular neoplasia. Hepatology. 2009 Feb;49(2):658–64.
29 Kitao A, Zen Y, Matsui O, Gabata T, Nakanuma Y. Hepatocarcinogenesis: multistep changes of drainage vessels at CT during arterial portography and hepatic arteriography--radiologic-pathologic correlation. Radiology. 2009 Aug;252(2):605–14.
30 Cheng MQ, Hu HT, Huang H, Pan JM, Xian MF, Huang Y, et al. Pathological considerations of CEUS LI-RADS: correlation with fibrosis stage and tumour histological grade. Eur Radiol. 2021 Aug;31(8):5680–8.
31 Schmilovitz-Weiss H, Tobar A, Halpern M, Levy I, Shabtai E, Ben-Ari Z. Tissue expression of squamous cellular carcinoma antigen and Ki67 in hepatocellular carcinoma-correlation with prognosis: a historical prospective study. Diagn Pathol. 2011 Dec 7;6:121.
32 Yang C, Su H, Liao X, Han C, Yu T, Zhu G, et al. Marker of proliferation Ki-67 expression is associated with transforming growth factor beta 1 and can predict the prognosis of patients with hepatic B virus-related hepatocellular carcinoma. Cancer Manag Res. 2018;10:679–96.
33 Menon SS, Guruvayoorappan C, Sakthivel KM, Rasmi RR. Ki-67 protein as a tumour proliferation marker. Clin Chim Acta. 2019 Apr;491:39–45.
34 Renzulli M, Brocchi S, Cucchetti A, Mazzotti F, Mosconi C, Sportoletti C, et al. Can current preoperative imaging Be used to detect microvascular invasion of hepatocellular carcinoma? Radiology. 2016 May;279(2):432–42.
35 Min JH, Lee MW, Park HS, Lee DH, Park HJ, Lim S, et al. Interobserver variability and diagnostic performance of gadoxetic acid-enhanced MRI for predicting microvascular invasion in hepatocellular carcinoma. Radiology. 2020 Dec;297(3):573–81.
36 Zhou H, Sun J, Jiang T, Wu J, Li Q, Zhang C, et al. A nomogram based on combining clinical features and contrast enhanced ultrasound LI-RADS improves prediction of microvascular invasion in hepatocellular carcinoma. Front Oncol. 2021;11:699290.
37 Terzi E, Giamperoli A, Iavarone M, Leoni S, De Bonis L, Granito A, et al. Prognosis of single early-stage hepatocellular carcinoma (HCC) with CEUS inconclusive imaging (LI-RADS LR-3 and LR-4) is No better than typical HCC (LR-5). Cancers. 2022 Jan 11;14(2):336.
38 Centonze L, De Carlis R, Vella I, Carbonaro L, Incarbone N, Palmieri L, et al. From LI-RADS classification to HCC pathology: a retrospective single-institution analysis of clinico-pathological features affecting oncological outcomes after curative surgery. Diagnostics. 2022 Jan 10;12(1):160.
39 An C, Park S, Chung YE, Kim DY, Kim SS, Kim MJ, et al. Curative resection of single primary hepatic malignancy: liver imaging reporting and data system category LR-M portends a worse prognosis. AJR Am J Roentgenol. 2017 Sep;209(3):576–83.
40 Rizvi S, Khan SA, Hallemeier CL, Kelley RK, Gores GJ. Cholangiocarcinoma: evolving concepts and therapeutic strategies. Nat Rev Clin Oncol. 2018 Feb;15(2):95–111.
41 Banales JM, Marin JJG, Lamarca A, Rodrigues PM, Khan SA, Roberts LR, et al. Cholangiocarcinoma 2020: the next horizon in mechanisms and management. Nat Rev Gastroenterol Hepatol. 2020 Sep;17(9):557–88.